THERMAL AND OPTICAL CHARACTERIZATION OF MATERIALS USING PHOTOACOUSTIC SPECTROSCOPY: AN INVERSE PROBLEM APPROACH

Antônio J. Silva Neto
Department of Mechanical Engineering and Energy, Instituto Politécnico, IPRJ,
Universidade do Estado do Rio de Janeiro, UERJ, CP 97282, 28601-970, Nova Friburgo, RJ, Brazil
ajsneto@iprj.uerj.br

Norberto Cella
Department of Materials, Instituto Politécnico, IPRJ
Universidade do Estado do Rio de Janeiro, UERJ, CP 97282, 28601-970, Nova Friburgo, RJ, Brazil
cella@iprj.uerj.br

Abstract. *In the present work we investigate the estimation of thermal and optical properties of materials using the photoacoustic technique. The direct problem is solved analitically using RG theory and the inverse problem is solved using the method of Levenberg-Marquardt. Good estimates and confidence bounds are obtained for the thermal diffusivity, the optical absorption coefficient and the thermal conductivity, when these parameters are estimated separately. Poor results were obtained for multiparameter estimation even for synthetic experimental data with low levels of noise.*

Keywords. *Photoacoustic spectroscopy, heat conduction, inverse problems, thermal characterization.*

1. Introduction

Photoacoustic Spectroscopy (PAS) is a very effective technique for nondestructive optical and thermal characterization of materials. Since the early work of Rosencwaig and Gersho (1976) it has gone throught a fast pace of development and the theorical physical grounds of the technique are now well established (McDonald and Wetsel, 1978, Mandelis et al. 1979, 1991, Rosencwaig, 1980, Vargas and Miranda, 1988, Mandelis and Hess, 1996, Hu et al., 1999, Gurevich et al., 2003).

Malkin and Cahen (1979) and Puchenkov (1995) looked into applications in photochemical and photobiological processes. Marquezini et al. (1991) performed spectroscopic studies of biological samples. Bodzenta et al. (2002) investigated the drug diffusion through membranes and the determination of parameters of diffusion for application in the pharmaceutical industry. Applications in atmospheric trace gases monitoring (Moeckli et al., 1998) and sea water properties determination (Mobley, 1994) have been reported.

A large number of publications is devoted to optical and thermal characterization of materials for applications in engineering. Just to mention a few examples, Leite et al. (1987) determined the thermal diffusivity of polymer foils, Calderón et al. (1997) measured the thermal diffusivity, and Bernini at al. (2003) measured the thermal conductivity of porous silicon, Zhao et al. (2000) reconstructed thermal conductivity depth profiles in laser-hardened aluminum alloys, and Power et al. (2000) and Fu and Power (2000) estimated depth profiles of heat source density and absorption coefficients in a number of materials with known properties in order to validate their methodology.

The photoacoustic effect is the basic phenomenon upon which PAS is built, and it occurs when a material sample placed inside a closed cell filled with air is illuminated with periodically interrupted light. The light absorbed by the sample is converted into heat through a nonradiative de-excitation process. The periodic flow of the heat into the air chamber of the cell produces, as an acoustic piston, pressure disturbances in it which can be detected by a microphone mounted at the cell wall. In the model developed by Rosencwaig and Gersho (1976), known as RG theory, this is the only phenomenon taken into account. Optical properties may be estimated through the understanding on how the light, or other electromagnetic radiation, is absorbed by the sample, while thermal properties may be obtained from the knowledge on how the heat diffuses through it.

PAS is now more generally referred to as Photothermal Spectroscopy because the thermal effect arises before the acoustic one when modulated electromagnetic radiation is absorbed by the material under analysis. However, when working with RG theory (Rosencwaig and Gersho, 1976), and a gas microphone as a signal detector, the old denomination PAS still holds.

Other phenomena besides the thermal diffusion may be responsible for the signal generation detected by the microphone. The cyclical expansion and contraction of the solid sample is described by the thermal expansion model (McDonald and Wetsel, 1978), and the cyclical thermoelastic bending of the solid sample due the variable absorption of the light with the depth of the sample is described by the thermoelastic bending model (Rousset et al., 1983).

Even when only one of the phenomena described above is taken into account, as is the case of the thermal diffusion in the RG theory, the analytical solution of the problem, if available, may become difficult to obtain and interpret. To make the problem more tractable special cases are examined for the sake of acquiring physical insight, but in such cases the applicability of the technique may be limited or even impaired. An alternative approach may be the use of numerical methods for the solution of the thermal diffusion equation (Goch and Reigl, 1996, Sampaio, 2001).

The inverse problem of optical and thermal properties estimation relies heavily on accurate physical, mathematical and computational modeling of the phenomena involved. Several methods have been developed for the solution of

inverse problems and some of them are described in the books by Tikhonov and Arsenin, (1977), Beck and Arnold (1977), Beck et al. (1985), Tarantola (1987), Alifanov (1995) and Alifanov et al. (1995), just to name a few.

In the last two decades the inverse heat transfer analysis has been widely used for the estimation of surface boundary conditions such as temperature or heat flux distributions (Alifanov, 1974, Su et al., 2000, Su and Silva Neto, 2001), material properties estimation (Silva Neto and Özisik, 1995, Silva Neto, 2002, Silva Neto and Soeiro, 2002, 2003), or heat sources intensity estimation (Silva Neto and Özisik, 1992, 1993, 1993a, 1994, Su and Silva Neto, 2001a, 2001b, Wang et al., 2002). A lot of effort is also observed in the use of the inverse problem approach in the development of the PAS technique (Mandelis et al., 1991, Power and Pristay, 1995, 1995a, Salnick and Mandelis, 1996, Power et al., 2000, Zhou et al., 2002, Power, 2002).

In the present work we use an implicit inverse problem formulation (Silva Neto, 2002) for the PAS with the direct problem modeled with the RG theory. For the solution of the direct problem the full analytical expression derived by Rosencwaig and Gersho (1976) is used. A higher computational effort is required, but by avoiding further approximations in the theoretical modeling better estimations for the material properties are expected.

The direct problem formulation with RG theory, and the inverse problem formulation and solution with the Levenberg-Marquardt method are described. Test case results are also presented.

2. Mathematical formulation and solution of the direct problem – RG theory

The RG theory is well described in the literature (Rosencwaig and Gersho, 1976, Rosencwaig, 1980), and consists on a one-dimensional model for the photoacoustic effect with the thermal diffusion being the dominant mechanism. Here we will just briefly reproduce the first part of the model up to the full expression for the real part of the complex temperature at the sample-air interface inside the photoacoustic cell.

Consider the closed cylindrical cell represented schematically in Fig. 1. The sample of the material under analysis is placed upon a backing material and the other boundary surface, adjoint to the air chamber of the cell, is exposed to an incident modulated light with intensity

$$I(t) = \frac{1}{2} I_0 \left(1 + \cos \omega t\right) \tag{1a}$$

where I_0 is the maximum intensity of the incident light, and ω is the angular frequency of the chopping mechanism.

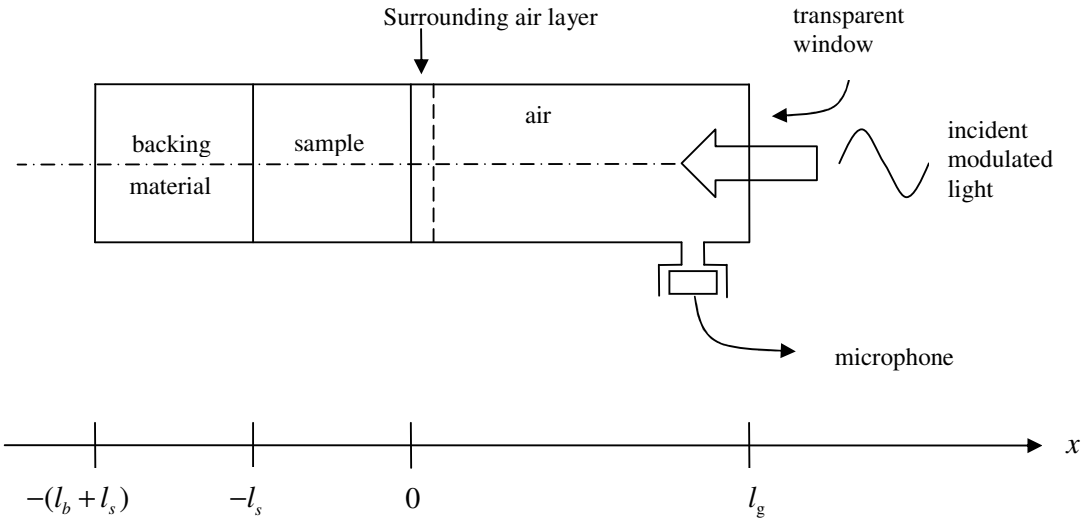

Figure 1 – Cross section of the photoacoustic cell.

It is assumed that the air is fully transparent to the light, and absorption occurs only at the sample according to Beer´s law

$$I(x,t) = e^{\beta x} I(t) \tag{1b}$$

such that the heat density $\left[W / m^3\right]$ produced is given by

$$F(x,t) = \frac{dI(x,t)}{dx} = \frac{1}{2} \beta I_0 e^{\beta x} \left(1 + \cos \omega t\right) \tag{2}$$

where β is the optical absorption coefficient.

In Fig. 1 l_s, l_g and l_b represent, respectively, the sample, air chamber and backing material thicknesses.

It is important to mention that the light intensity is considered uniform upon all the surface of the sample, and the absorbed light is completely converted into thermal energy.

With the heat source modeled by Eq. (2) the heat diffusion problem in the cell is mathematically formulated as

$$\frac{\partial^2\theta_g(x,t)}{\partial x^2}=\frac{1}{\alpha_g}\frac{\partial\theta_g(x,t)}{\partial t},\quad 0<x<l_g \tag{3a}$$

$$\frac{\partial^2\theta_s(x,t)}{\partial x^2}=\frac{1}{\alpha_s}\frac{\partial\theta_s(x,t)}{\partial t}-\frac{\beta I_0}{2k_s}e^{\beta x}\left(1+e^{j\omega t}\right),\quad -l_s<x<0 \tag{3b}$$

$$\frac{\partial^2\theta_b(x,t)}{\partial x^2}=\frac{1}{\alpha_b}\frac{\partial\theta_b(x,t)}{\partial t},\quad -(l_b+l_s)<x<-l_s \tag{3c}$$

with the interface conditions

$$\theta_s(0,t)=\theta_g(0,t) \tag{3d}$$

$$\theta_s(-l_s,t)=\theta_b(-l_s,t) \tag{3e}$$

$$k_s\left.\frac{\partial\theta_s(x,t)}{\partial x}\right|_{x=0}=k_g\left.\frac{\partial\theta_g(x,t)}{\partial x}\right|_{x=0} \tag{3f}$$

$$k_s\left.\frac{\partial\theta_s(x,t)}{\partial x}\right|_{x=-l_s}=k_b\left.\frac{\partial\theta_b(x,t)}{\partial x}\right|_{x=-l_s} \tag{3g}$$

and initial conditions

$$\theta_g(x,0)=0,\quad 0\le x\le l_g \tag{3h}$$

$$\theta_s(x,0)=0,\quad -l_s\le x\le 0 \tag{3i}$$

$$\theta_b(x,0)=0,\quad -(l_s+l_b)\le x\le -l_s \tag{3j}$$

where j is the imaginary number $\sqrt{-1}$, θ is the complex-valued temperature, k represents the thermal conductivity, α the thermal diffusivity, and the subscripts g, s and b denotes air (gas), sample and backing material, respectively.

As we substitute the term $\cos\omega t$ in Eqs. (1,2) by the term $e^{j\omega t}$ in Eq. (3b), only the real part of the complex temperature $\theta(x,t)$, i.e. $\mathrm{Re}\left[\theta(x,t)\right]$, has physical meaning. The actual temperature field in the cell is given by

$$T(x,t)=\mathrm{Re}\left[\theta(x,t)\right]+T_{amb} \tag{4}$$

where T_{amb} is the ambient temperature.

After a short period of time a steady periodic state is established. Considering

$$\mathrm{Re}\left[\theta\left(-(l_b+l_s),t\right)\right]=0 \quad \text{and} \quad \mathrm{Re}\left[\theta\left(l_g,t\right)\right]=0 \tag{5}$$

and ignoring the convective heat transfer from the sample to the air chamber, the general solution of Eqs. (3a-c) is given by (Rosencwaig and Gersho, 1976)

$$\theta(x,t)=\begin{cases}\dfrac{1}{l_b}\left(x+l_s+l_b\right)W_0+We^{\sigma_b(x+l_s)}e^{j\omega t},\ -\left(l_b+l_s\right)\le x\le -l_s & \text{(6a)}\\ b_1+b_2x+b_3e^{\beta x}+\left(Ue^{\sigma_s x}+Ve^{-\sigma_s x}-Ee^{\beta x}\right)e^{j\omega t},\ -l_s\le x\le 0 & \text{(6b)}\\ \left(1-\dfrac{x}{l_{\mathrm{g}}}\right)F_0+\theta_0e^{-\sigma_g x}e^{j\omega t},\ 0_s\le x\le 1_{\mathrm{g}} & \text{(6c)}\end{cases}$$

where the complex thermal diffusion coefficient is given by

$$\sigma=(1+j)a \tag{6d}$$

and a is the thermal diffusion coefficient

$$a=\left(\frac{\omega}{2\alpha}\right)^{\frac{1}{2}} \tag{6e}$$

In Eqs. (6a-c) b_1, b_2, b_3, W_0, and F_0 are real valued constants, and W, U, V, E, and θ_0 are complex valued constants. F_0 and W_0 denote the time-independent (dc) component of the solution, at $x=0$ and $x=-l_s$, respectively. θ_0 and W denote the time-dependent (ac) component of the solution, at $x=0$ and $x=-l_s$, respectively.

The quantities b_3 and E are determined by the particular solution of Eq. (3b) and are given by

$$b_3=-\frac{I_0}{2k_s\beta} \tag{7a}$$

$$E=\frac{\beta I_0}{2k_s\left(\beta^2-\sigma_s^2\right)} \tag{7b}$$

Applying the interface conditions (3d-g) separately to the dc (real) and ac (complex) constants we get the following expressions

$$b_1=-\left[\frac{\left(l_bk_s+l_sk_b\right)\left(k_g+l_gk_s\beta\right)+l_gk_s\left(k_b-l_bk_s\beta\right)e^{-\beta l_s}}{\left(l_bk_s+l_sk_b\right)k_g+l_gk_bk_s}\right]b_3 \tag{8a}$$

$$b_2=-\left[\frac{k_g\left(b_1+b_3\right)}{l_gk_s}+\beta b_3\right] \tag{8b}$$

$$W_0=-\frac{l_b}{k_b}\left[\frac{k_g\left(b_1+b_3\right)}{l_{\mathrm{g}}}+\beta b_3k_s-k_s\beta b_3e^{-\beta l_s}\right] \tag{8c}$$

$$F_0=b_1+b_3 \tag{8d}$$

$$V=\left[\frac{(1-b)(g+r)e^{-\sigma_s l_s}+(b-r)(g+1)e^{-\beta l_s}}{(1-b)(g-1)e^{-\sigma_s l_s}+(b+1)(g+1)e^{\sigma_s l_s}}\right]E \tag{9a}$$

$$W=-\left[\frac{e^{-\sigma_s l_s}(g-1)}{(g+1)}+\sigma_sk_s\right]V+\left[\frac{e^{-\sigma_s l_s}(g+r)}{(g+1)}-k_s\beta\right]E \tag{9b}$$

$$U=-\frac{(g-1)}{(g+1)}V+\frac{(g+r)}{(g+1)}E \tag{9c}$$

$$\theta_0 = \left[\frac{(r-1)(b+1)e^{\sigma_s l_s} - (r+1)(b-1)e^{-\sigma_s l_s} + 2(b-r)e^{-\beta l_s}}{(g+1)(b+1)e^{\sigma_s l_s} - (g-1)(b-1)e^{-\sigma_s l_s}} \right] E \tag{9d}$$

where

$$b = \frac{k_b a_b}{k_s a_s} \quad \text{and} \quad g = \frac{k_g a_g}{k_s a_s} \tag{10a,b}$$

are real valued and

$$r = \frac{(1-j)\beta}{2a_s} \tag{10c}$$

is complex valued.

The derivation presented here follows closely the one developed by Rosencwaig and Gersho (1976), except that here are explicitly given all coefficients appearing in Eqs. (6a-c). The main goal of Rosencwaig and Gersho was to obtain the solution for the coefficient θ_0 that represents the complex amplitude of the periodic temperature at the solid-air interface, i.e. at $x = 0$. We have a broader interest in determining the spatial and time dependence of temperature in order to allow a future comparison of the analytical solution with a numerical one, and that is the reason why we gave the full solution (6a-c). Nonetheless this is still a on going project, and therefore for the inverse problem formulation and solution that will be presented in the next section we have also worked only with the solution $\theta(x,t)$ at the sample-air interface, i.e. $x = 0$.

Rosencwaig and Gersho (1976) went a step further avoiding the complexity of Eqs. (6a-c) by considering particular cases within the context of the two extreme situations: (i) optically transparent solids; and (ii) optically opaque solids. In the present work we are not tied up to such limitations.

When the geometry, the optical and thermal properties, and the initial and boundary conditions are all known, we have the so called direct problem, and then Eqs. (6a-c) provide the temperature distribution as a function of space and time.

3. Mathematical formulation and solution of the inverse problem

Using the photoacoustic cell represented schematically in Fig. 1 we are interested in determing the thermal conductivity, k_s, the thermal diffusivity, α_s, and the optical absorption coefficient, β.

For each modulation frequency f_k, $k = 1, 2, ..., N_f$, where $f_k = \omega_k / 2\pi$, we consider to be available experimental data on the temperature at the interface sample-air, i.e. $\theta_0(f_k, t)$. As $\theta_0(f_k, t)$ is complex valued, we get information from both the amplitude $A(f_k)$ and the phase-lag $\Phi(f_k)$. In the present work we consider information only related to the amplitude $A(f_k)$, $k = 1, 2, ..., N_f$, as shown in Fig. 2.

In our investigation we consider the following vectors of unknowns

$$\vec{Z}_1 = \{\alpha\}; \quad \vec{Z}_2 = \{\beta\}; \quad \vec{Z}_3 = \{k\}; \quad \vec{Z}_4 = \{\alpha, k\}^T \quad \text{and} \quad \vec{Z}_5 = \{\alpha, \beta, k\}^T \tag{11}$$

where T denotes transpose.

As the number of available data, N_f, will be larger than the number of unknowns, M, the inverse problem is formulated implicitly as an optimization one (Silva Neto, 2002), and we seek to minimize the squared residues functional

$$S(\vec{Z}) = \sum_{k=1}^{N_f} \left[A_{calc}(f_k, \vec{Z}) - A_{\exp}(f_k) \right]^2 = \vec{F}^T \vec{F} \tag{12}$$

where A_{calc} and $A_{\exp}$ are the calculated and experimental values for the amplitude of the steady periodic temperature at $X = 0$, and the elements of the vector of residues are

$$F_k = A_{calc}\left(f_k, \vec{Z}\right) - A_{\exp}\left(f_k\right), \quad k = 1, 2, ..., N_f \tag{13}$$

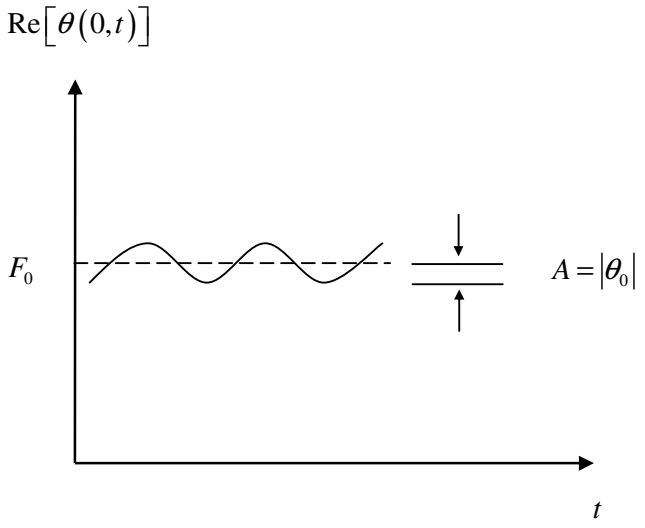

Figure 2 – Amplitude of the steady periodic temperature at $x = 0$.

In order to find the vector $\vec{Z}$ that gives the best fit in Eq. (12) we look for the minimization of functional S. The first step is then to write the critical point equation that yields the system of nonlinear equations

$$\frac{\partial S}{\partial Z_m} = \frac{\partial}{\partial Z_m}\left(\vec{F}^T \vec{F}\right) = 0, \quad m = 1, 2, ..., M \tag{14}$$

Equation (14) leads to

$$J^T \vec{F}\left(\vec{Z}\right) = 0 \tag{15}$$

where the elements of the Jacobian matrix are given by

$$J_{pq} = \frac{\partial A_{calc}\left(f_p, \vec{Z}\right)}{\partial Z_q}, \quad p = 1, 2, ..., N_f \quad \text{and} \quad q = 1, 2, ..., M \tag{16}$$

Using a Taylor´s expansion

$$\vec{F}\left(\vec{Z}^{n+1}\right) = \vec{F}\left(\vec{Z}^n + \Delta\vec{Z}^n\right) = \vec{F}\left(\vec{Z}^n\right) + \sum_{s=1}^{M} \left.\frac{\partial \vec{F}\left(\vec{Z}\right)}{\partial Z_s}\right|_{\vec{Z}^n} \Delta\vec{Z}_s^n + \mathcal{O}\left(\Delta\vec{Z}^2\right) = \vec{F}\left(\vec{Z}^n\right) + J^n \Delta\vec{Z}^n + \mathcal{O}\left(\Delta\vec{Z}^2\right) \tag{17}$$

introducing Eq. (17) into Eq. (15), keeping only the terms up to the first order, and adding a damping factor λ^n to the elements of the diagonal of matrix $J^T J$ to improve convergence, we obtain a variation of the least-squares method known as the Levenberg-Marquard method (Marquardt, 1963)

$$\left(J^{n^T} J^n + \lambda^n I\right)\Delta\vec{Z}^n = -J^{n^T} \vec{F}^n \tag{18}$$

where n now becomes an iteration index, and *I* is the identity matrix. Starting with an initial guess for the vector of unknowns, $\vec{Z}^o$, new estimates are obtained with

$$\vec{Z}^{n+1} = \vec{Z}^n + \Delta\vec{Z}^n, \quad n = 0,1,2,... \tag{19}$$

The iterative procedure described by Eq. (19) is interrupted when a stopping criterion is satisfied, e.g.

$$\left|\frac{\Delta Z_s^n}{Z_s^n}\right| < \varepsilon, \quad s = 1,2,...,M \tag{20}$$

where ε is a tolerance, say 10^{-5}.

The elements of the Jacobian matrix given by Eq. (16) as well as the righ hand term of Eq. (18) were calculated using the direct problem solution described in the previous section.

3.1 Confidence Bounds

The confidence bounds for the estimates $\vec{Z}$ are calculated using the procedure developed by Gallant (1987). Using the notation employed by Huang and Özisik (1990)

$$\sigma_{\vec{Z}} = \sigma\left\{diag\left[\frac{\partial\vec{A}_{calc}^T}{\partial\vec{Z}}\frac{\partial\vec{A}_{calc}}{\partial\vec{Z}^T}\right]^{-1}\right\}^{\frac{1}{2}} \tag{21}$$

where $\vec{A}_{calc}$ is the vector containing the elements $\vec{A}_{calc}(f_k)$, $k = 1,2,...,N_f$, and σ is the standard derivation of the measurement errors.

Assuming a normal distribution for the experimental errors, and 99% of confidence, the confidence bounds for the estimates Z_s, $s = 1,2,...,M$, are calculated by (Flach and Özisik, 1989)

$$\left[Z_s - 2{,}576\sigma_{Z_s}, Z_s + 2{,}576\sigma_{Z_s}\right], \quad s = 1,2,...,M \tag{22}$$

4. Results and discussion

This work is part of an ongoing research project, and our final goal is to use real experimental data that will be acquired with the photoacoustic apparatus available in our institution. But, before dealing with additional difficulties associated with the experimental work we decided to do a pure numerical investigation. Therefore, the "synthetic" experimental data was generated using

$$A_{\exp}(f_k) = A_{calc}(f_k, \vec{Z}_{exact}) + 2.576\, r\, \sigma \tag{23}$$

where r is a random number in the range $-1 \le r \le 1$, and σ represents the standard deviation of the measurement errors.

Also looking a step forward, i.e. the coupling with the experimental work, the backing and sample materials, the cell dimensions and the parameters associated with the modulated source of light used here represent a real practical situation. The values for all these parameters are given in Table 1.

4.1 Estimation of the sample thermal diffusivity α_s

In order to validate the methodology implemented for the inverse problem solution we first run test cases with noiseless data, i.e. $\sigma = 0$ in Eq. (23).

Using initial guesses in the range $10^{-8} m^2/s \le \alpha_s^0 \le 5.0\times10^{-6} m^2/s$ the algorithm converged to the exact value $\alpha_s = 5.286\times10^{-7} m^2/s$, even with $\lambda^n = 0$ in Eq. (18), requiring only up to 6 iterations. For $\alpha_s^0 = 10^{-5} m^2/s$, we used $\lambda^0 = 10$ and the algorithm converged for the exact result in 16 iterations.

We then perturbed the calculated values of the amplitude in Eq. (23) by using $\sigma = 5\times10^{-5}$ which yielded up to $10\,\%$ error in the values of $A_{\exp}(f_k)$. Using the initial guess $\alpha_s^0 = 5.0\times10^{-6} m^2/s$ and $\lambda^n = 0$ good estimates and small confidence bounds were obtained as shown in Fig. 3a. Each run represents a different set of random numbers being used in Eq. (23), simulating then different experimental runs.

Table 1 – Parameters for the sample material and photoacoustic cell.

backing material	Aluminum, $\alpha_b = 0.82\times10^{-4} m^2/s$, $k_b = 201 W/mK$, $l_b = 5\times10^{-3} m$
sample	Opaque glass, $\alpha_s = 5.286\times10^{-7} m^2/s$, $\beta = 10^3 m^{-1}$, $k_s = 1.047 W/mK$, $l_s = 5\times10^{-3} m$
gas	Air, $\alpha_g = 1.9\times10^{-4} m^2/s$, $k_g = 0.0239 W/mK$, $l_g = 1.2\times10^{-3} m$
light	Laser HeNe or other monochromatic light, $I_0 = 100 W/m^2$ modulation frequencies used $f = 10, 11, ..., 17 Hz$

4.2 Estimation of the sample optical absorption parameter β

Using noiseless data and initial guess values within the range $10 m^{-1} \le \beta^0 \le 10^2 m^{-1}$, convergence to the exact value $\beta = 10^3 m^{-1}$ was achieved within 6 iterations of the iterative procedure, even with $\lambda^n = 0$. For the initial guess $\beta^0 = 5\times10^3 m^{-1}$ and $\beta^0 = 10^4 m^{-1}$ convergence was obtained in 6 iterations using $\lambda^0 = 10^{-8}$.

We then used $\sigma = 5\times10^{-5}$ in Eq. (23), going up to $15\,\%$ error in the synthetic experimental data. Five test cases were run using the same initial guess $\beta^0 = 5\times10^3 m^{-1}$ and $\lambda^0 = 10^{-8}$. The results obtained are shown in Fig. 3b. Good results were obtained for the estimates as well as small confidence bounds.

4.3 Estimation of the sample thermal conductivity k_s

Using noiseless data and initial guess values within the range $4.0\times10^{-2} W/mK \le k_s^0 \le 2.0\ W/mK$ convergence to the exact value $k_s = 1.047 W/mK$ was achieved within 14 iterations of the iterative procedure, even with $\lambda^n = 0$. For the initial guess $k_s^0 = 4.0\ W/mK$ convergence was obtained in 8 iterations using $\lambda^0 = 10^{-2}$. For the initial guess $k_s^0 = 20\ W/mK$ convergence was not obtained even for a wide range of values for λ^0. We decided then to use a reduction factor in the correction of the estimates in Eq. (19). Instead of adding $\Delta\vec{Z}^n$ to $\vec{Z}^n$ in order to obtain $\vec{Z}^{n+1}$, we used $\gamma\,\Delta\vec{Z}^n$ were $\gamma < 1$. Therefore, with $\lambda^n = 0$ and $\gamma = 0.05$ convergence was achieved with 80 iterations.

With $\sigma = 2.5\times10^{-5}$ we got up to $10\,\%$ error in the experimental data. Five test cases were run using the same initial guess $k_s^0 = 4.0\ W/mK$ and $\lambda^0 = 10^{-2}$. The results obtained are shown in Fig. 3c. Good results were obtained for the estimates and confidence bounds.

4.4 Simultaneous estimation of α_s and k_s

A test case was run with $\sigma = 0$, and convergence to the exact values $\alpha_s = 5.286\times10^{-7} m^2/s$ and $k_s = 1.047 W/mK$ was achieved with 6 iterations using $\alpha_s^0 = 10^{-6} m^2/s$, $k_s^0 = 2.0\ W/mK$ and $\lambda^n = 0$.

We then performed tests with noisy data. Poor estimates for both parameters, α_s and k_s, were obtained even for small levels of noise. As an example, with $\sigma = 10^{-6}$, representing $0.3\,\%$ of error in experimental data, the following results were obtained in two different runs: (1) $\alpha_s = 5.222\ [1.771\ ;\ 8.674] \times 10^{-7}\, m^2/s$ and $k_s = 1.034\ [0.3691\ ;\ 1.699]\ W/mK$; and (2) $\alpha_s = 4.375\ [1.208\ ;\ 7.543] \times 10^{-7}\, m^2/s$ and $k_s = 0.8706\ [0.2556\ ;\ 1.486]\ W/mK$.

4.5 Simultaneous estimation of α_s, β and k_s

Even with noiseless data the simultaneous estimation of the three parameters was not possible, at least for the practical situation and sets of parameters we worked with.

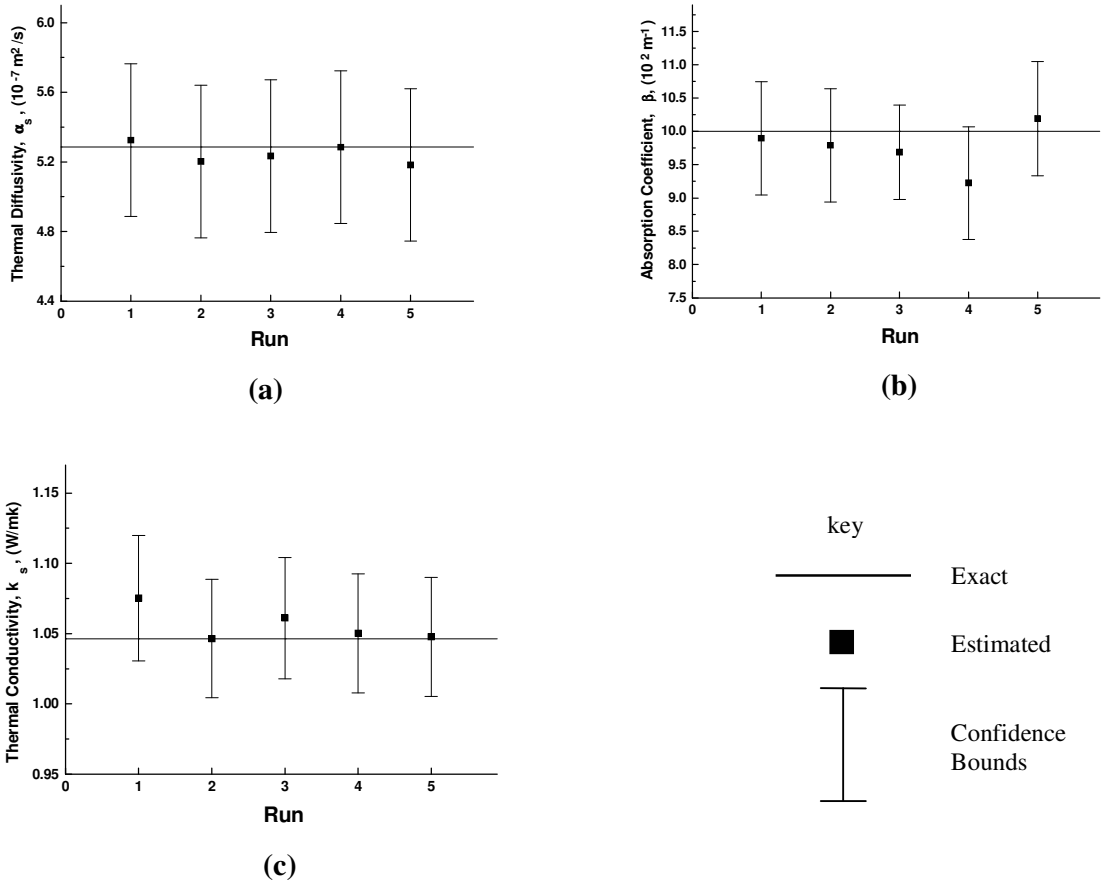

Figure 3 – Results for the estimated parameters (a) α_s, (b) β and (c) k_s.

5. Conclusions

The analytical solution obtained with RG theory and the Levenberg-Marquardt method yielded good estimates for thermal and optical parameters estimated separately in a photoacoustic spectroscopy simulated experiment. When multiparameter estimation is attempted poor results are obtained even for low levels of noise in the experimental data. In our future steps we will investigate the use of the information provided by the phase lag $\phi(f_k)$ of the temperature at the sample-air interface.

Acknowledgements

The authors acknowledge the financial support provided by CNPq and FAPERJ.

References

Alifanov, O.M. Inverse Heat Transfer Problems, Springer Verlag, 1995.

Alifanov, O. M., Artyukhin, E. A. and Rumiantsev, S. V., Extreme Methods for Solving Ill-Posed Problems with Applications to Inverse Heat Transfer Problems, Begell House, 1995.

Alifanov, O.M., Solution of an Inverse Problem of Heat Conduction by Iteration Methods, Journal of Engineering Physics, Vol. 26, pp. 471-476, 1974.

Beck, J. V. and Arnold, K. J., Parameter Estimation in Engineering and Science, Wiley, 1977.

Beck, J. V., Blackwell, B. and St. Clair Jr., C. R., Inverse Heat Conduction, Wiley, 1985.

Bernini, U., Lettiere, S., Massera, E. and Rucco, P. A., Investigation of Thermal Transport in *n*-Type Porous Silicon by Photo-Acoustic Technique, Optics and Lasers in Engineering, Vol. 39, pp. 127-140, 2003.

Bodzenta, J., Bukowski, R. J., Christ, A. and Pogoda, T., Photoacoustic Detection of Drug Diffusion into a Membrane: Theory and Numerical Analysis, International Journal of Heat and Mass Transfer, Vol. 45, pp. 4515-4523, 2002.

Calderón, A., Alvarado-Gil, J. J., Gurevich, Y. G., Cruz-Orea, A., Delgadillo, I., Vargas, H. and Miranda, L. C. M, Photothermal Characterization of Electrochemical Etching Processed *n*-Type Porous Silicon, Physical Review Letters, Vol. 79, No. 25, pp. 5022-5025, 1997.

Flach, G. P. and and Özisik, M. N., Inverse Heat Conduction Problem of Simultaneously Estimating Spatially Varying Thermal Conductivity and Heat Capacity per Unit Volume, Numerical Heat Transfer, Vol. 16, pp. 249-266, 1989.

Fu, S. W. and Power, J. F., Depth Profiling of Optical Absorption in Thin Films via the Mirage Effect and a New Inverse Scattering Theory. Part II: Experimental Reconstruction on Well-Characterized Materials, Applied Spectroscopy, Vol. 54, No. 1, pp. 127-137, 2000.

Gallant, A. R., Nonlinear Statistical Models, Wiley, 1987.

Goch, G. and Reigl., M., Application of the Finite-Element Method and the Finite-Difference Method to Photothermal Inspections, Journal of Applied Physics, Vol. 79, No. 12, pp. 9084-9089, 1996.

Gurevich, Y. G, Logvinov, G. N., de la Cruz, G. G. and López, G. E., Physics of Thermal Waves in Homogenous and Inhomogeneous (Two-Layer) Samples, International Journal of Thermal Sciences, Vol. 42, pp. 63-69, 2003.

Hu, H., Wang, X. and Xu, X., Generalized Theory of the Photoacoustic Effect in a Multilayer Material, Journal of Applied Physics, Vol. 86, No. 7, pp 3953-3958, 1999.

Huang, C. H. and Özisik, M. N., A Direct Integration Approach for Simultaneously Estimating Spatially Varying Thermal conductivity and Heat Capacity, International Journal of Heat and Fluid Flow, Vol. 11, pp 262-268, 1990.

Leite, N. F., Cella, N., Vargas, H. and Miranda, L. C. M, Photoacoustic Measurement of Thermal Diffusivity of Polymer Foils, Journal of Applied Physics, Vol. 61, No. 8, pp. 3025-3027, 1987.

Malkin, S. and Cahen, D., Photoacoustic Sectroscopy and Radiant Energy – Convertion – Theory of the Effect with Special Emphasis on Photosynthesis, Photochemistry and Photobiology, Vol. 29, No. 4, pp. 803-813, 1979.

Mandelis, A., Peralta, S. and Thoen, J., Photoacoustic Frequency-Domain Depth Profiling of Continuously Inhomogeneous Condensed Phases: Theory and Simulations for the Inverse Problem, Journal of Applied Physics, Vol. 70, No. 3, pp.1761-1770, 1991.

Mandelis, A. and Hess, P., Life and Earth Sciences, Progress in Photothermal and Photoacoustic Science and Technology, Vol. 3, SPIE Optical Engineering Press, 1996.

Mandelis, A., Teng, Y. C. and Royce, B. S. H, Phase Measurements in the Frequency Domain Photoacoustic Spectroscopy of Solids, Journal of Applied Physics, Vol. 50, No. 11, pp. 7138-7146, 1979.

Marquardt, D. W., An Algorithm for Least-Squares Estimation of Nonlinear Parameters, Journal of the Society for Industrial and Applied Mathematics, Vol. 11, pp. 431-441, 1963.

Marquezini, M. V., Cella, N., Mansanares, A. M., Vargas, H. and Miranda, L.C.M., Open Photoacoustic Cell Spectroscopy, Measurement Science and Technology, Vol. 2, pp. 396-401, 1991.

McDonald, F. A. and Wetsel Jr. G. C., Generalized Theory of the Photoacoustic Effect, Journal of Applied Physics, Vol. 49, No. 4, pp. 2313-2322, 1978.

Mobley, C. D., Light and Water – Radiative Transfer in Natural Waters, Academic Press, 1994.

Moeckli, M. A., Hilbes, C. and Sigrist, M. W., Photoacustic Multicomponent Gas Analysis Using a Levenberg-Marquardt Fitting Algorithm, Applied Physics B-Lasers and Optics, Vol. 67, pp. 449-458, 1998.

Power, J. F. and Prystay, M. C., Expectation Minimum (EM): A New Principle for the Solution for Ill-Posed Problems in Photothermal Science, Applied Spectroscopy, Vol. 49, No. 6, pp. 709-724, 1995.

Power, J. F. and Prystay, M. C., Nondestructive Optical Depth Profiling in Thin Films through Robust Inversion of the Laser Photopyroeletric Effect Impulse Response, Applied Spectroscopy, Vol. 49, No. 6, pp. 725-746, 1995a.

Power, J. F., Fu, S. W. and Schweitzer, M. A., Depth Profiling of Optical Absorption in Thin Films via the Mirage Effect and a New Inverse Scattering Theory. Part I: Principles and Methodology, Applied Spectroscopy, Vol. 54, No 1, pp. 110-126, 2000.

Power, J. F., Inverse Problem Theory in the Optical Depth Profilometry of Thin Films, Review of Scientific Instruments, Vol. 73, No 12, pp. 4057-4140, 2002.

Puchenkov, O. V., Photoacoustic Diagnostics of Fast Photochemical and Photobiological Process. Analysis of Inverse Problem Solotion, Biohphysical Chemistry, Vol. 56, pp. 241-261, 1995.

Rosencwaig, A. and Gersho, A., Theory of the Photoacoustic Effect with Solids, Journal of Applied Physics, Vol. 47, No. 1, pp. 64-69, 1976.

Rosencwaig, A., Photoacoustics and Photoacoustic Spectroscopy, Wiley, 1980.

Rousset, G., Lepoutre, F. and Bertrand, L., Influence of Thermoeplastic Bending on Photoacoustic Experiments Related to Measurements of Thermal Diffusivity of Metals, Journal of Applied Physics, Vol. 54, No.5, pp. 2383-2391, 1983.

Salnick, A. and Mandelis, A., Hamiltonian Plasma-Harmonic Oscillator Theory: Generalized Depth Profilometry of Electronically Continuously Inhomogeneous Semiconductors and the Inverse Problem, Journal of Applied Physics, Vol. 80, No 9, pp 5278-5288, 1996.

Sampaio, M. S., Aplicação do Método dos Elementos Finitos ao Efeito Fototérmico para a Determinação da Difusividade Térmica, M. S. Dissertation, Instituto Politécnico, UERJ, 2001.

Silva Neto, A. J., Explicit and Implicit Formulations for Inverse Radiative Transfer Problems, 5th World Congress on Computacional Mechanics, Mini-Symposium MS125- Computational Treatment of Inverse Problems in Mechanics, Vienna, Austria, 2002.

Silva Neto, A. J. and Özisik, M. N., Two-Dimensional Inverse Heat Conduction Problem of Estimating the Time – Varying Strength of a Line Heat Source, Journal of Applied Physics, Vol. 71, No. 11, pp. 5357-5362, 1992.

Silva Neto, A. J. and Özisik, M. N., Simultaneous Estimation of Location and Timewise Varying Strenght of a Plane Heat Source, Numerical Heta Transfer – Part A: Applications, Vol. 24, pp. 467-477, 1993.

Silva Neto, A. J. and Özisik, M. N., Inverse Problem of Simultaneously Estimating the Timewise – Varying Strengths of Two Plane Heat Sources, Journal of Applied Physics, Vol. 73, No. 5, pp. 2132-2137, 1993a.

Silva Neto, A. J. and Özisik, M. N., The Estimation of Space and Time Dependent Strength of a Volumetric Heat Source in a One-Dimensional Plate, International Journal of Heat and Mass Transfer, Vol. 37, No. 6, pp. 909-915, 1994.

Silva Neto, A. J. and Özisik, M. N., An Inverse Problem of Simultaneous Estimation of Radiation Phase Function, Albedo and Optical Thickness, Journal of Quantitative Spectroscopy and Radiative Transfer, Vol. 53, No. 4, pp. 397-409, 1995.

Silva Neto, A. J. and Soeiro, F. J. C. P., Estimation of Phase Function of Anisotropic Scattering with a Combination of Gradient Based and Stochastic Global Optimization Methods, 5th World Congress on Computational Mechanics, Vienna, Austria, 2002.

Silva Neto, A. J. and Soeiro, F. J. C. P., Solution of Implicitly Formulated Inverse Heat Transfer Problems with Hybrib Methods, Mini-Symposium Inverse Problems from Thermal / Fluids and Solid Mechanics Appications – 2nd MIT Conference on Computational Fluid and Solid Mechanics, Cambridge, USA, 2003.

Su, J. and Silva Neto, A. J., Simulation Estimation of Inlet Temperature and Wall Heat Flux in Turbulent Circular Pipe Flow, Numerical Heat Transfer – Part A: Applications, Vol. 40, No. 7, pp. 751-766, 2001.

Su, J. and Silva Neto, A. J., Two-Dimensional Inverse Heat Conduction Problem of Source Strength Estimation in Cylindrical Rods, Applied Mathematical Modeling, Vol. 25, pp. 861-872, 2001a.

Su, J. and Silva Neto, A. J., Heat Source Estimation with the Conjugate Gradient Method in Inverse Linear Diffusive Problems, Journal of the Brazilian Society of Mechanical Sciences, Vol. XXIII, No. 3, pp. 321-334, 2001b.

Su, J., Lopes, A. B. and Silva Neto, A. J., Estimation of Unknown Wall Heat Flux in Turbulent Circular Pipe Flow, International Communications in Heat Mass Transfer, Vol. 27, No.7, pp. 945-954, 2000.

Tarantola, A., Inverse Problem Theory: Methods for Data Fitting and Model Parameter Estimation, Elsevier, 1987.

Tikhonov, A. N. and Arsenin, V. Y., Solutions of Ill-Posed Problems, Wiley, 1977.

Vargas, H. and Miranda, L. C. M., Photoacoustic and Related Photothermal Techniques, Physics Reports, Vol. 161, No. 2, pp. 43-101, 1988.

Wang, J., Silva Neto, A. J., Moura Neto, F. D. and Su, J., Function Estimation with Alifanov´s Iterative Regularization Method in Linear and Nonlinear Heat Conduction Problems, Applied Mathematical Modelling, Vol. 26, No. 11, pp. 1093-1111, 2002.

Zhao, Y. Z., Zhang, S. Y., Cheng, J. C., Zhang, Y. K. and Xu, W.H., Depth Profile Reconstruction of the Thermal Conductivity of Inhomogeneous Solids: Application to Laser-Hardened Al Alloys, Applied Physics A – Materials Science & Processing, Vol. 71, pp. 319-323, 2000.

Zhou, Q. B., Lu, Y. K., Zhang, S. Y., Cheng, J. C. and Shui, X. J. Two-Dimensional Reconstruction Theory of Thermal Conductivity Profiles Based on the Thermal Wave Technique, Journal of Applied Physics, Vol. 92, No. 7, pp. 4088-4094, 2002.